

# Fabrication and compressive strength of porous hydroxyapatite scaffolds with a functionally graded core/shell structure

Young-Mi Soon<sup>a</sup>, Kwan-Ha Shin<sup>a</sup>, Young-Hag Koh<sup>a,\*</sup>, Jong-Hoon Lee<sup>b</sup>,  
Won-Young Choi<sup>b</sup>, Hyoun-Ee Kim<sup>b</sup>

<sup>a</sup> Department of Dental Laboratory Science and Engineering, Korea University, Seoul 136-703, Republic of Korea

<sup>b</sup> Department of Materials Science and Engineering, Seoul National University, Seoul 151-742, Republic of Korea

Received 7 June 2010; received in revised form 26 August 2010; accepted 6 September 2010

Available online 29 September 2010

## Abstract

A novel type of porous hydroxyapatite (HA) scaffolds with a functionally graded core/shell structure was fabricated by freeze casting HA/camphene slurries with various HA contents into fugitive molds containing a graphite template with three-dimensionally interconnected pores for the creation of a highly porous core. All the fabricated samples had functionally graded core/shell structures with 3-D periodic pore networks in a core surrounded by a relatively dense shell. The overall porosity of the sample decreased from 60 to 38 vol% with increasing HA content in the HA/camphene slurry from 20 to 36 vol% due to a decrease in porosity in both the core and shell regions. In addition, the compressive strength was improved remarkably from  $12 \pm 1.1$  to  $32 \pm 3.0$  MPa. The *in vitro* cell test using a pre-osteoblast cell line showed that the samples had good biocompatibility.

© 2010 Elsevier Ltd. All rights reserved.

**Keywords:** : Suspensions; Porosity; Mechanical properties; Apatite; Biomedical applications

## 1. Introduction

Functionally graded materials (FGMs) with a gradient of properties have attracted recent interest, owing to their superior mechanical and biological properties to conventional porous materials.<sup>1–9</sup> For example, it was reported that hydroxyapatite (HA) scaffolds with a porosity gradient mimicking the architecture of natural bone could induce rapid bone ingrowth into the high-porosity portion and withstand physiological mechanical stress through the low-porosity portion, when implanted.<sup>1</sup> Thus far, a variety of manufacturing methods for the production of FGMs have been developed, including the utilizations of multiple and differentiated impregnations,<sup>1</sup> multiple tape casting,<sup>3</sup> modified sponge replication method,<sup>5</sup> injected molding,<sup>7</sup> and freeze casting.<sup>8,9</sup> However, the development of new manufacturing methods that can tightly control the gradient of properties in a cost-effective manner is still a challenge.

This paper demonstrates the utility of the camphene-based freeze casting for the production of porous hydroxyapatite (HA) scaffolds with a functionally graded core/shell structure. To accomplish this, a fugitive mold consisting of a graphite template with three-dimensionally interconnected pores and a square mold was prepared, as illustrated in Fig. 1(A). Subsequently, HA/camphene slurries with various HA contents, ranging from 20 to 36 vol%, were freeze-cast into the fugitive molds at room-temperature, followed by freeze drying and sintering at 1250 °C for 3 h. This simple method allowed the formation of a highly porous core with a three-dimensional periodic pore network, surrounded by a relatively dense shell, as shown in Fig. 1(B). In addition, a porosity gradient could be created by controlling the HA content in the HA/camphene slurry. The fabricated samples were characterized by considering their porous structures, such as the overall porosity, pores formed both in the core and shell regions, as well as the densification of the HA walls. The crystalline phases of the samples were examined by X-ray diffraction (XRD). The compressive strength of the samples was also assessed to determine their structural integrity. The preliminary osteoblastic activity of the samples was also evaluated using *in vitro* tests to determine their biocompatibility.

\* Corresponding author. Tel.: +82 2 940 2844; fax: +82 2 909 3502.  
E-mail address: [kohyh@korea.ac.kr](mailto:kohyh@korea.ac.kr) (Y.-H. Koh).

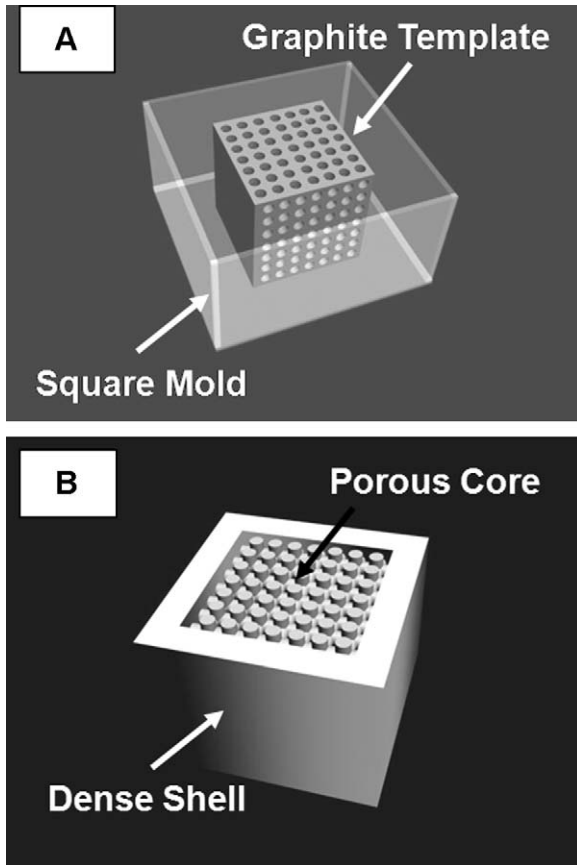


Fig. 1. Schematic diagrams showing (A) the fugitive mold used to produce the porous HA scaffolds with a functionally graded core/shell structure and (B) the resulting HA scaffold with a functionally graded core/shell structure.

## 2. Experimental procedure

Porous hydroxyapatite (HA) scaffolds with a functionally graded core/shell structure were produced by freeze casting HA/camphene slurries into fugitive molds. First, a graphite template was prepared by machining solid graphite, 13 mm × 13 mm × 13 mm in size, using a mini-CNC machine according to a predetermined design. The graphite template contained tightly controlled pores, 1 mm in diameter, with a fixed distance between the 0.7 mm pores. A fugitive mold was then prepared by assembling the graphite template with a square polymeric mold (see Fig. 1(A)).

Commercially available HA powder ( $\text{Ca}_{10}(\text{PO}_4)_6(\text{OH})_2$ ; Alfa Aesar Co., Milwaukee, WI, USA) and camphene ( $\text{C}_{10}\text{H}_{16}$ ; Alfa Aesar/Avocado Organics, Ward Hill, MA, USA) were used as the ceramic powder and freezing vehicle, respectively. In particular, the as-received HA powders were calcined at 1000 °C for 1 h to reduce the specific surface area, which would be expected to improve the rheological properties of the HA/camphene slurry.<sup>10</sup> The HA/camphene slurries with various HA contents (20, 25, 30, and 36 vol%) were prepared by dispersing the HA powders in molten camphene by ball-milling at 60 °C for 24 h using an oligomeric polyester (Hypermer KD-4; UniQema, Everburg, Belgium) as a dispersant at 3 wt%. Subsequently, the warm slurries prepared were poured into the fugitive molds at

room-temperature and then kept at this temperature for 1 h to allow complete solidification. After demolding, the green bodies, ~20 mm × 20 mm × 13 mm in size, were freeze dried to remove the solid camphene. The green samples were then heated at 900 °C for 3 h to remove the graphite template and dispersant completely, followed by subsequent heat-treatment at 1250 °C for 3 h to sinter the HA walls.

The porous structures (e.g., overall porosity, pores formed both in the core and shell regions, and densifications of the HA walls) of the fabricated samples were observed by scanning electron microscopy (FE-SEM, JSM-6330F, JEOL Techniques, Tokyo, Japan). The crystalline phases of the samples were characterized by X-ray diffraction (XRD, M18XHF-SRA, MacScience Co., Yokohama, Japan). For the compressive strength tests, the samples with dimensions of ~16 mm × 16 mm × 10 mm, which had been prepared by slightly grinding their top and bottom surfaces were loaded at a crosshead speed of 5 mm/min using a screw driven load frame (Instron 5565, Instron Corp., Canton, MA, USA). The stress and strain responses of the samples were monitored during the compressive strength tests. Five samples were tested to obtain an average value and standard deviation.

The *in vitro* cell tests of the samples were performed using a pre-osteoblast cell line (MC3T3-E1; ATCC, CRL-2593, USA). The cells were plated at a density of  $5 \times 10^4$  cells/mL and cultured in a humidified incubator in an atmosphere containing 5%  $\text{CO}_2$  at 37 °C. Minimum essential medium ( $\alpha$ -MEM; Welgene Co., Ltd., Seoul, Korea) supplemented with 10% fetal bovine serum (FBS; Life Technologies, Inc., USA) and 1% penicillin–streptomycin was used as the culturing medium. The cell attachment was observed by SEM after culturing for 1 day.

## 3. Results and discussion

The freeze casting of HA/camphene slurries into fugitive molds was used to produce porous hydroxyapatite (HA) scaffolds with a functionally graded core/shell structure. In particular, a highly porous core with a three-dimensional periodic pore network was achieved using a graphite template that could be removed by thermal oxidation.<sup>11</sup> In addition, it was possible to create porosity gradients in the samples, in which the microstructures and porosity of the shells were controlled by adjusting the initial HA content in the HA/camphene slurry, ranging from 20 to 36 vol%, which would enable tailoring of their mechanical properties. In other words, compressive strength would increase with increasing HA content due to the lower porosity of the shell.<sup>12,13</sup>

Fig. 2(A) shows an optical micrograph of the samples produced with an initial HA content of 30 vol% before and after sintering at 1250 °C for 3 h. Regardless of the initial HA content, it was possible to infiltrate the HA/camphene slurries into the graphite template with three-dimensionally interconnected pores. This consequently endowed the samples with a tightly controlled pore structure after sintering. However, a HA content >36 vol% hindered the complete infiltration of the slurry into the pores formed in the graphite template owing to its high viscosity. All the fabricated samples showed similar linear shrinkage

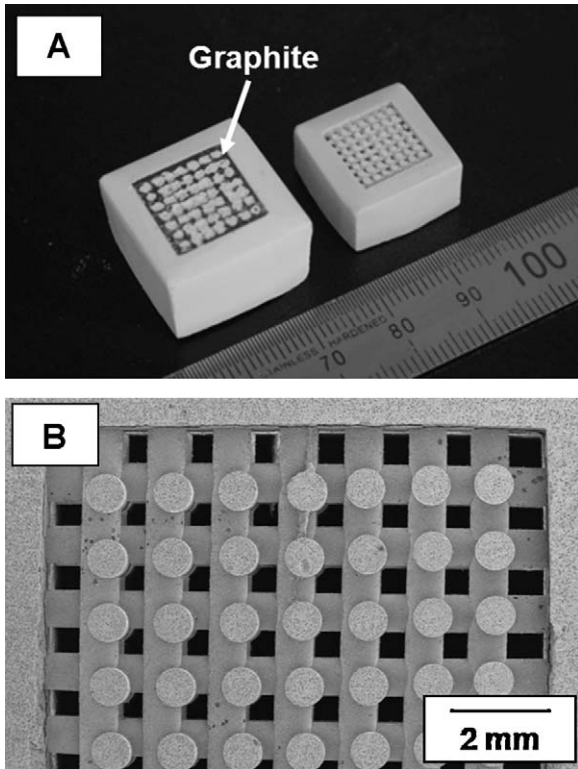


Fig. 2. (A) Typical optical micrograph of the freeze-cast sample (left) and fabricated scaffold after sintering at 1250 °C for 3 h (right) and (B) typical SEM image of the porous HA scaffold, showing the core/shell structure. The initial HA content in the slurry was 30 vol%.

of ~20% after sintering, as well as good shape tolerance due to the complete removal of the graphite template without causing any noticeable defects, such as cracking and distortion, which would be troublesome for conventional polymeric templates.<sup>11</sup>

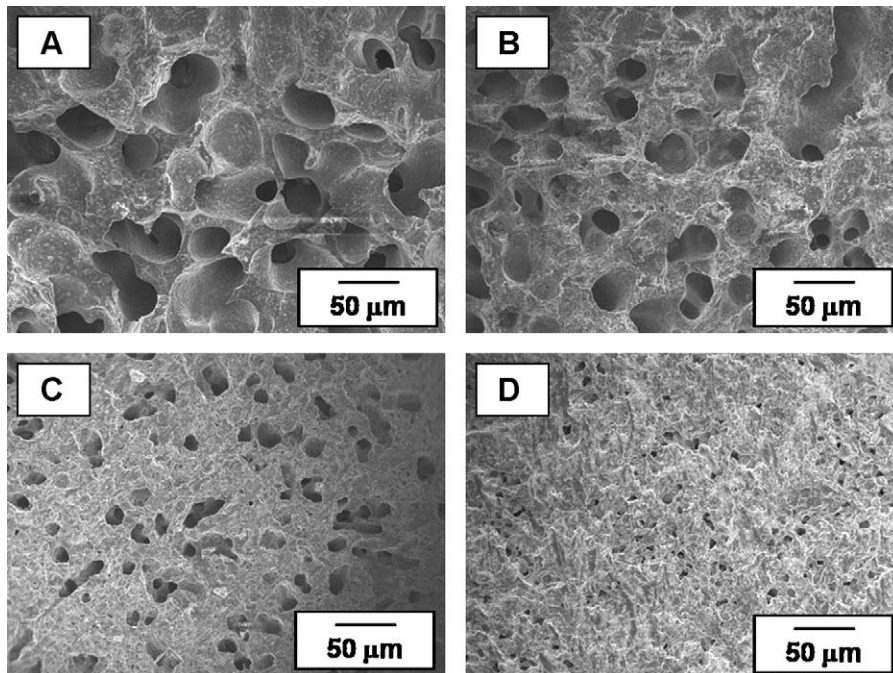


Fig. 3. SEM images of the HA shells produced with various initial HA contents: (A) 20 vol%, (B) 25 vol%, (C) 30 vol% and (D) 36 vol%.

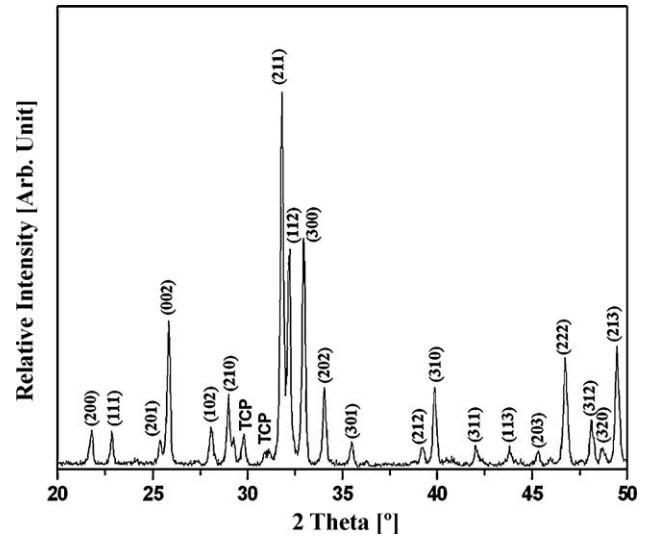


Fig. 4. Typical XRD pattern of the sample produced with a HA content of 36 vol% after sintering at 1250 °C for 3 h. The peaks of crystalline HA phase are indexed (TCP, tri-calcium phosphate).

Fig. 2(B) shows clearly the construction of periodic pores in the core surrounded by the relatively dense shell. The distance between the HA walls formed in the core was approximately 546 μm, which would be expected to provide a favorable environment for bone ingrowth.<sup>13,14</sup> This pore size can be tuned simply by adjusting the distance between the pore formed in the graphite template. In addition, the sample showed good bonding between the core and shell regions.

One of the most striking features of the present method is the ability to control the microstructure and porosity of the shell simply by adjusting the initial HA content employed in the HA/camphene slurry.<sup>10,15</sup> As expected, the porosity and pore

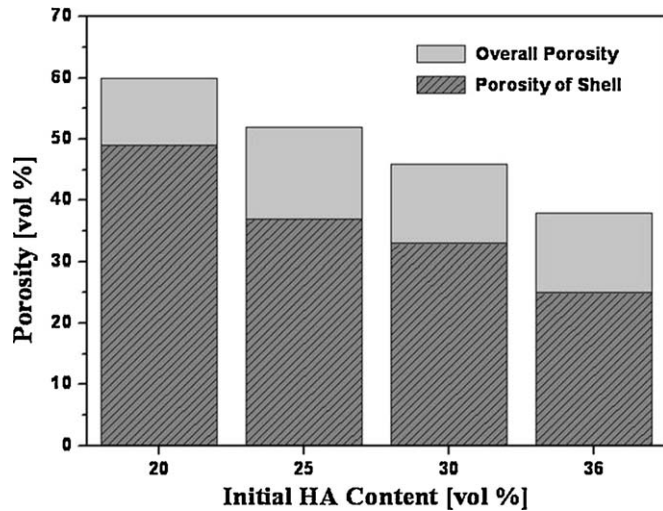


Fig. 5. Overall porosity of the porous HA scaffolds and porosity of the shell as a function of the initial HA content.

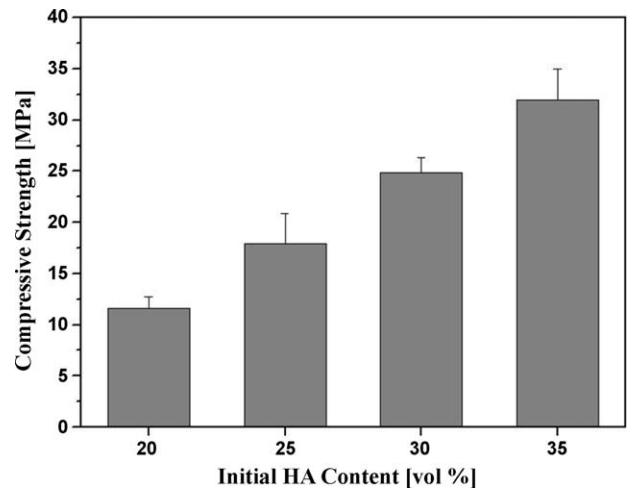


Fig. 6. Compressive strength of the porous HA scaffolds as a function of the initial HA content.

size decreased notably with increasing HA content, as shown in Fig. 3(A)–(D). When a HA content of 20 vol% was used, the shell showed a highly porous structure with a number of pores, several tens of microns in size, formed as a replica of the camphene dendrites (Fig. 3(A)).<sup>10,12,15</sup> The sample produced with a HA content of 25 vol% still showed high porosity but with a smaller pore size (Fig. 3(B)). These interconnected pores would be expected to stimulate the attachment, proliferation, and differen-

tiation of bone cells.<sup>14</sup> On the other hand, distinctively different microstructures were observed, when the HA content exceeded 30 vol%, i.e., relatively small pores were formed (Fig. 3(C)). The decrease in porosity and pore size became more obvious when the HA content was increased to 36 vol%, in which only small closed pores were formed throughout the sample (Fig. 3(D)).

The crystalline structures of the sample were examined by XRD. All samples showed similar XRD patterns, regardless of the initial HA content in the HA/camphene slurries. Fig. 4

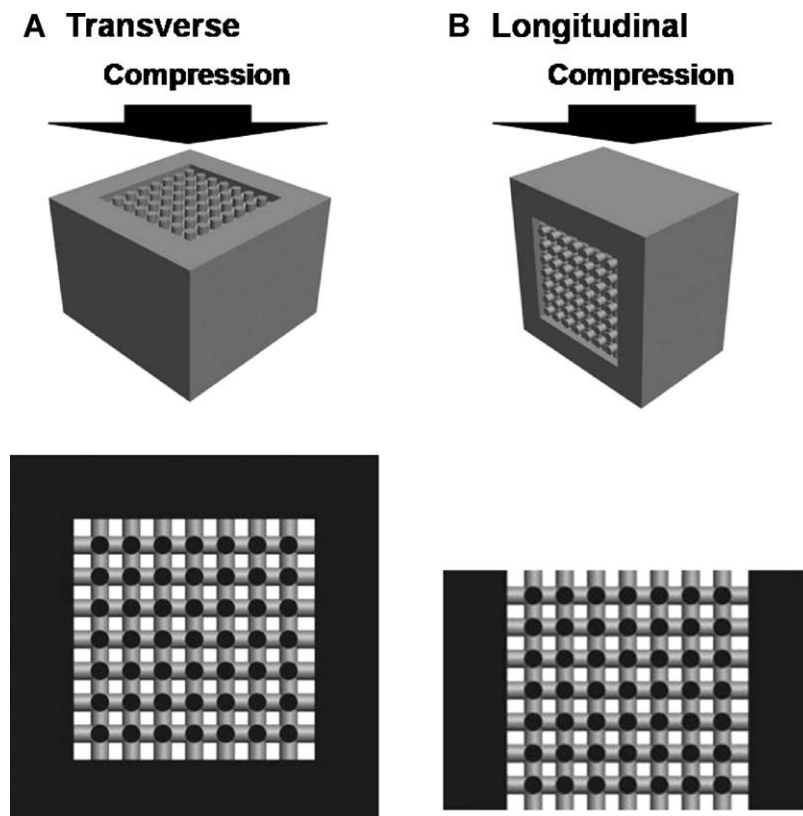


Fig. 7. Schematic diagrams showing the mechanical responses of the porous HA scaffold with a functionally graded core/shell structure when compressed (A) transversely and (B) longitudinally. The black regions represent the actual parts that can endure an applied load.

shows a typical XRD pattern of the sample produced with a HA content of 36 vol%. The strong peaks corresponded well to those of hydroxyapatite crystal (JCPDS file No. 9-432). In addition, peaks associated with crystalline  $\beta$ -tricalcium phosphate ( $\beta$ -TCP) were also detected as a secondary phase (JCPDS file No. 9-169), which would presumably be related to the oxidation of the graphite mold. However, it should be noted that both materials, i.e., HA and TCP, are osteoconductive.<sup>16</sup>

The overall porosity of the samples was calculated by measuring their weight and dimensions. As the HA content was increased from 20 to 36 vol%, the overall porosity decreased significantly from 60 to 38 vol%, as shown in Fig. 5. This reduction was attributed mainly to a decrease in the porosity of the shell. Therefore, the porosity of the shells separated from the samples was also calculated by measuring their weight and dimensions. The porosity of the shell was decreased from 49 to 25 vol%, with increasing initial HA content from 20 to 36 vol%, corresponding to the SEM observations.

The compressive strengths of the samples were measured to evaluate their structural integrity. Basically, regardless of the initial HA content, all the samples fabricated showed similar brittle fracture behaviors. That is, a linear increase in stress with an elastic response followed by a rapid decrease due to the fast fracture of the relatively dense shell.<sup>17</sup> The compressive strength was increased remarkably from  $12 \pm 1.1$  to  $31 \pm 3$  MPa, with increasing initial HA content from 20 to 36 vol%, as shown in Fig. 6, which is due mainly to the decrease in shell porosity.<sup>10,13,14</sup>

The mechanical properties of the HA scaffold with a functionally graded core/shell structure can be estimated roughly by considering the fractions of the HA parts that are normal to the direction of the applied load.<sup>17</sup> In other words, the compressive strength of the HA scaffold ( $\sigma_{\text{Scaffold}}$ ) can be expressed as follows:

$$\sigma_{\text{Scaffold}} = \frac{\sigma_{\text{Porous HA}}}{(A/A_0)} \quad (1)$$

where  $\sigma_{\text{Porous HA}}$  represents the compressive strength of the porous HA, whereas  $A$ , which is marked by black area in Fig. 7(A) and (B), and  $A_0$  are the active resisting area and total cross-sectional area of the scaffold, respectively. The  $A/A_0$  value is calculated to be 0.674 by considering the geometry of the scaffold when compressed transversely (Fig. 7(A)). This suggests that the compressive strength of the HA scaffold should be 67.4% of that of the porous HA. However, the scaffold can retain only 32.4% of the porous HA when compressed longitudinally (Fig. 7(B)). Therefore, the mechanical properties of the HA scaffolds with a core/shell structure should be interpreted carefully for actual applications as a bone scaffold. In addition, other factors, including the pore geometry and size, should be considered for the precise modeling of the mechanical behavior.<sup>18</sup>

The preliminary osteoblastic activity of the samples was evaluated with an *in vitro* test using a pre-osteoblast cell line. Regardless of the initial HA content, all the fabricated samples showed good biocompatibility without any sign of cytotoxicity, i.e., the cells adhered and spread actively on the samples. Fig. 8(A) and (B) shows a typical SEM image of the cells cul-

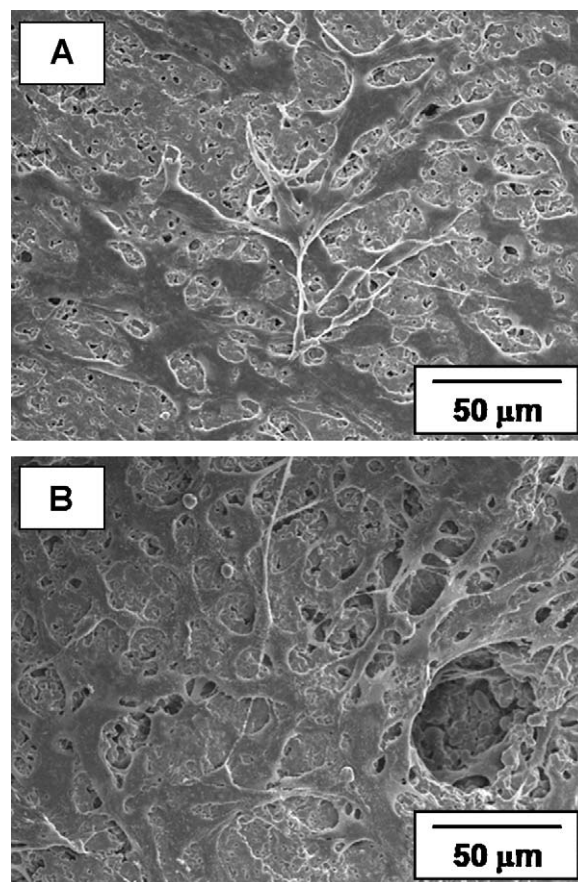


Fig. 8. Typical SEM images of the cells cultured for 1 day (A) on the core and (B) on the shell of the sample produced with a HA content of 36 vol%.

tured for 1 day on the core and shell regions of the sample produced with a HA content of 36 vol%, respectively. The cells appeared to grow and spread actively both on the core and shell regions, indicating that the porous HA scaffolds with a functionally graded core/shell structure have good biocompatibility.

#### 4. Conclusions

Camphene-based freeze casting was used to produce porous hydroxyapatite (HA) scaffolds with a functionally graded core/shell structure, wherein the core contained a three-dimensional (3-D) periodic pore networks formed by the removal of a graphite template, surrounded by a relatively dense shell. Furthermore, the microstructures and porosities of the shells were controlled by adjusting the initial HA content used in the HA/camphene slurries, consequently creating porosity gradients in the samples. The overall porosity of the sample and the porosity of the shell decreased from 60 to 38 vol% and from 49 to 25 vol%, respectively, with increasing HA content from 20 to 36 vol%. These decreases produced remarkable improvements in compressive strength. The sample produced with a HA content of 36 vol% showed high compressive strength of  $31 \pm 3$  MPa with a porosity of 38 vol%, as well as a highly porous core with 3-D periodic pore networks,  $\sim 546 \mu\text{m}$  in size, which would provide a favorable environment for bone ingrowth, as suggested by the *in vitro* cell tests.

## Acknowledgment

This work was supported by the Korea Science and Engineering Foundation (KOSEF) grant funded by the Korea government (MEST) (No. 2009-0073415).

## References

1. Tampieri A, Celotti G, Sprio S, Delcogliano A, Franzese S. Porosity-graded hydroxyapatite ceramics to replace natural bone. *Biomaterials* 2001;**22**:1365–70.
2. Thieme M, Wieters KP, Bergner F, Scharnweber D, Worch H, Ndop J, et al. Titanium powder sintering for preparation of a porous functionally graded material destined for orthopaedic implants. *J Mater Sci: Mater Med* 2001;**12**:225–31.
3. Werner J, Linner-Krčmar B, Friess W, Greil P. Mechanical properties and in vitro cell compatibility of hydroxyapatite ceramics with graded pore structure. *Biomaterials* 2002;**23**:4285–94.
4. Kieback B, Neubrand A, Riedel H. Processing techniques for functionally graded materials. *Mater Sci Eng A* 2003;**362**:81–105.
5. Hsu YH, Turner IG, Miles AW. Fabrication of porous bioceramics with porosity gradients similar to the bimodal structure of cortical and cancellous bone. *J Mater Sci: Mater Med* 2007;**18**:2251–6.
6. Zhang YP, Li DS, Zhang XP. Gradient porosity and large pore size NiTi shape memory alloys. *Scripta Mater* 2007;**57**:1020–3.
7. Zhang F, Chang J, Lu J, Lin K, Ning C. Bioinspired structure of bioceramics for bone regeneration in load-bearing sites. *Acta Biomater* 2007;**3**:896–904.
8. Macchetta A, Turner IG, Bowen CR. Fabrication of HA/TCP scaffolds with a graded and porous structure using a camphene-based freeze-casting method. *Acta Biomater* 2009;**5**:1319–27.
9. Jung HD, Yook SW, Kim HE, Koh YH. Fabrication of titanium scaffolds with porosity and pore size gradients by sequential freeze casting. *Mater Lett* 2009;**63**:1545–7.
10. Lee EJ, Koh YH, Yoon BH, Kim HE, Kim HW. Highly porous hydroxyapatite bioceramics with interconnected pore channels using camphene-based freeze casting. *Mater Lett* 2007;**61**:2270–3.
11. Jun IK, Koh YH, Song JH, Kim HE. Fabrication and characterization of dual-channeled zirconia ceramic scaffold. *J Am Ceram Soc* 2006;**89**:2021–6.
12. Yoon BH, Koh YH, Park CS, Kim HE. Generation of large pore channels for bone tissue engineering using camphene-based freeze casting. *J Am Ceram Soc* 2007;**90**:1744–52.
13. Karageorgiou V, Kaplan D. Porosity of 3D biomaterial scaffolds and osteogenesis. *Biomaterials* 2005;**26**(27):5474–91.
14. Hing KA. Bioceramic bone graft substitutes: influence of porosity and chemistry. *Int J Appl Ceram Technol* 2005;**2**:184–99.
15. Araki K, Halloran JW. Porous ceramic bodies with interconnected pore channels by a novel freeze casting technique. *J Am Ceram Soc* 2005;**88**:1108–14.
16. Huttmacher DW, Schantz JT, Lam CX, Tan KC, Lim TC. State of the art and future directions of scaffold-based bone engineering from a biomaterials perspective. *J Tissue Eng Regen Med* 2007;**1**:245–60.
17. Gibson LJ. Biomechanics of cellular solids. *J Biomech* 2005;**38**:377–99.
18. Hattiangadi A, Bandyopadhyay A. Strength degradation of nonrandom porous ceramic structures under uniaxial compressive loading. *J Am Ceram Soc* 2000;**8**:2730–6.